

TRIPLET EXCITON TRANSPORT IN THE  
BENZOPHENONE-FLUORENE-NAPHTHALENE MOLECULE

by

Duncan C. McElfresh

**© Copyright by Duncan C. McElfresh, 2013**

All Rights Reserved

A thesis submitted to the Faculty and the Board of Trustees of the Colorado School of Mines in partial fulfillment of the requirements for the degree of Master of Science (Applied Physics).

Golden, Colorado

Date \_\_\_\_\_

Signed: \_\_\_\_\_

Duncan C. McElfresh

Signed: \_\_\_\_\_

Dr. Mark T. Lusk  
Thesis Advisor

Golden, Colorado

Date \_\_\_\_\_

Signed: \_\_\_\_\_

Dr. Thomas E. Furtak  
Department Head  
Department of Physics

## ABSTRACT

Incoherent triplet-triplet energy transfer through the benzophenone-fluorene-naphthalene system is computationally investigated to determine triplet hopping rates. These rates have been previously measured experimentally and have also been estimated computationally. There are many complex steps associated with such a computational analysis, though, and earlier efforts resorted to a variety of semi-empirical modifications to the methods used in order to obtain results consistent with the experimental data. This has motivated an investigation in which best practice methods are applied to the system without any empirical adjustments. The calculation of triplet excitation energy and triplet-triplet electronic coupling are examined in detail using a range of computational methods from simple Density Functional Theory to the many-body Green function approach embodied in the Bethe-Salpeter Equation. This analysis includes an evaluation of the robustness of each method considered. Significantly, the investigation identifies the excited states of benzophenone as being extremely difficult to calculate using even the most advanced excitation methods, and a theory is presented as to why the molecule is both interesting and troublesome. The final rate estimates, without any empirical adjustments, are one to two orders of magnitude greater than those measured experimentally. This data, and the detailed methodological study supporting it, is expected to be helpful in future efforts to computationally scrutinize triplet exciton hopping.

## TABLE OF CONTENTS

ABSTRACT . . . . .	iii
LIST OF FIGURES . . . . .	vi
LIST OF TABLES . . . . .	vii
LIST OF SYMBOLS . . . . .	viii
LIST OF ABBREVIATIONS . . . . .	ix
ACKNOWLEDGMENTS . . . . .	xi
DEDICATION . . . . .	xii
CHAPTER 1 INTRODUCTION . . . . .	1
1.1 The <i>Bp-F-Nap</i> Molecule . . . . .	3
1.2 Experimental Benchmark . . . . .	4
1.3 Computational Benchmark . . . . .	5
CHAPTER 2 THEORY . . . . .	6
2.1 Diabatic and Adiabatic States . . . . .	6
2.2 Density of States . . . . .	9
2.2.1 FCWD . . . . .	10
2.3 Electronic Coupling . . . . .	11
2.3.1 Hartree-Fock Coupling – Diabatic States . . . . .	12
2.4 Fragment Spin Difference – Adiabatic States . . . . .	13
2.5 Driving Force $\Delta G$ . . . . .	15
2.5.1 Reorganization Energy . . . . .	15

2.6	Ground State Electronic Structure Calculations . . . . .	16
2.6.1	Exchange-Correlation Functionals . . . . .	17
2.6.2	Excited State Electronic Structure Calculations . . . . .	18
CHAPTER 3 COMPUTATIONAL IMPLEMENTATION: OPTICAL GAP . . . . .		22
3.1	Discussion . . . . .	25
3.2	Discussion – Benzophenone . . . . .	26
CHAPTER 4 COMPUTATIONAL IMPLEMENTATION: COUPLING . . . . .		32
4.1	Discussion – Coupling . . . . .	34
CHAPTER 5 COMPUTATIONAL IMPLEMENTATION: REORGANIZATION ENERGY . . . . .		37
5.1	Discussion . . . . .	37
CHAPTER 6 RESULTS AND DISCUSSION: TTET RATES . . . . .		39
6.1	Final FGR Parameters . . . . .	39
6.2	Final Rates and Discussion . . . . .	41
CHAPTER 7 DISCUSSION AND CONCLUSIONS . . . . .		43
REFERENCES CITED . . . . .		48

## LIST OF FIGURES

Figure 1.1	FCWD for the $Bp \rightarrow F$ Transition . . . . .	3
Figure 1.2	The $Bp$ - $F$ - $Nap$ molecule . . . . .	4
Figure 2.1	Diabatic and adiabatic PESs . . . . .	8
Figure 2.2	FCWD for the $Bp \rightarrow F$ transition . . . . .	11
Figure 2.3	Comparison of GW and DFT (LDA) optical gaps . . . . .	20
Figure 3.1	Phenalenone molecule . . . . .	29
Figure 3.2	$Bp$ molecule . . . . .	29
Figure 6.1	Modal reorganization energies $\lambda_i$ and Huang-Rhys factors $S_i$ . . . . .	40
Figure 6.2	FCWD for $Bp$ , $F$ , and $Nap$ . . . . .	41

## LIST OF TABLES

Table 3.1	Triplet DFT HOMO-LUMO gaps (eV) . . . . .	23
Table 3.2	Triplet BSE energies, for geometries optimized into the LDA and PBE ground and triplet states (eV) . . . . .	23
Table 3.3	Triplet TDDFT energies, PBE-ground-state geometry (eV) . . . . .	24
Table 3.4	Triplet TDDFT energies, PBE-excited-state geometry (eV) . . . . .	24
Table 3.5	Triplet CIS energies, for geometries optimized into the PBE ground and triplet states (eV) . . . . .	25
Table 3.6	Mulliken populations on benzophenone oxygen . . . . .	28
Table 3.7	Lowest triplet energy of <i>Bp</i> , by angle between benzene rings . . . . .	30
Table 3.8	Lowest CIS and CISD energies of <i>Bp</i> . . . . .	30
Table 4.1	HF coupling calculations for the <i>Bp</i> → <i>F</i> transition (meV) . . . . .	33
Table 4.2	FSD coupling calculations, on both the complete <i>Bp-F-Nap</i> molecule, and its constituent dimers (meV) . . . . .	35
Table 4.3	FSD coupling calculations for the <i>Bp-me</i> → <i>F</i> transition (meV), calculated on the <i>Bp-F</i> dimer . . . . .	35
Table 5.1	Reorganization energies for hopping transitions (eV) . . . . .	37
Table 6.1	Final Rate Parameters . . . . .	39
Table 6.2	Final Hopping Rate Calculations, at 300K ( $10^{10}$ Hz) . . . . .	41

## LIST OF SYMBOLS

Driving force . . . . .	$\Delta G$
Density of States . . . . .	$\rho$
Reorganization Energy . . . . .	$\lambda$
Electronic Coupling . . . . .	$V_{da}$

## LIST OF ABBREVIATIONS

Triplet-Triplet Energy Transport . . . . .	TTET
Hartree-Fock . . . . .	HF
Fragment Spin Difference . . . . .	FSD
Bethe-Salpeter Equations . . . . .	BSE
Fermi's Golden Rule . . . . .	FGR
Density of States . . . . .	DOS
benzophenone-fluorene-naphthalene . . . . .	<i>Bp-F-Nap</i>
Density Functional Theory . . . . .	DFT
Time-Dependent Density Functional Theory . . . . .	TDDFT
Configuration Interaction Singles . . . . .	CIS
Constrained Density Functional Theory . . . . .	CDFT
Potential Energy Surface . . . . .	PES
Franck-Condon Weighted Density of States . . . . .	FCWD
Electron Volt . . . . .	eV
Highest Occupied Molecular Orbital . . . . .	HOMO
Lowest Unoccupied Molecular Orbital . . . . .	LUMO
GW Quasiparticle Theory . . . . .	GW
Exchange-Correlation . . . . .	XC
Local Density Approximation . . . . .	LDA
Generalized Gradient Approximation . . . . .	GGA

Quantum Mechanics/Molecular Mechanics . . . . . QM/MM

## ACKNOWLEDGMENTS

Foremost, I would like to thank my advisor Dr. Mark Lusk. His kind patience and dedication has granted me a purchase on knowledge that I never thought possible. I would also like to thank the entire electronic structure group, and especially Huashan Li, for politely answering and re-answering my questions – even on late nights and weekends.

This thesis research was made possible by funding from the SMART scholarship and the United States Department of Defense, which has afforded me financial stability throughout this degree program.

This work is dedicated to my family, whose unwavering support has driven me to accomplish even my craziest dreams.

# CHAPTER 1

## INTRODUCTION

Triplet-triplet exciton transport (TTET) is an important mechanism in many fields of research. Unlike singlet excitations, triplets do not quickly decay back into the ground state, as this transition is spin-forbidden. This affords triplets an extremely long lifetime relative to singlet excitations, making them very useful in energy transport applications. TTET has also been shown to play a key role in biological and chemical processes, such as photosynthesis and photosensitization [1]. Attempts are being made to harness the usefulness of triplets found in nature, and apply them to technologies such as photovoltaics and organic electronics [2]. In order to design and study these technologies, we must first understand TTET from a theoretical perspective; this is still an open area of research.

This thesis examines best practice computational approaches for studying incoherent TTET through the benzophenone-fluorene-naphthalene system. Although there is now a large body of experimental research measuring TTET rates [3], the computational and theoretical methods used to study this process are not well established because such rate estimates call for a number of sophisticated calculations of excited state molecular assemblies that tend to be extremely sensitive to environmental and geometric uncertainty. These investigations typically include a variety of semi-empirical corrections intended to bring computational results more in line with experimental measurements. Frustratingly, such corrections are often unexplained or weakly supported, making them suspect if only because they result in predictions that match experimental data extremely well.

One difficulty of TTET calculations is the electronic coupling. Coupling interactions used in singlet energy transport, such as Förster resonant energy transport, rely on the Coulomb interaction; however this interaction is spin-forbidden for TTET, so other coupling methods must be used. There have been multiple new TTET coupling methods proposed recently,

such as Hartree-Fock (HF) coupling [4] and the fragment-spin-difference (FSD) method [5], which are studied in this thesis. Yet there has been no study of the accuracy or robustness of these methods, making them unreliable for use in predictive analyses. This thesis endeavors to study and compare the HF and FSD coupling methods, and to discuss how and to what extent they can be used to predict TTET rates.

Another difficulty of TTET is the calculation of triplet excitation energies, which determine the driving force  $\Delta G$  of the hopping process. Time-dependent density functional theory (TDDFT) and more recently the Bethe-Salpeter equations (BSE) have been used to successfully improve the calculation of excitation energies [6, 7]. Yet these sophisticated methods have not yet been proven to be reliable; TDDFT excitation energies can differ from experimental values by up to 1 eV [8], and the BSE method still requires extensive testing.

A third difficulty in producing computational results that can be compared with experimental data is that rate calculations are very sensitive to the excitation energies involved in hopping. This makes it extremely important to estimate these energies accurately. In Fermi's golden rule (FGR) [9], the hopping rate is directly proportional to the density of states (DOS). Most DOSs are a Gaussian or Lorentzian function of the driving force, making them extremely sensitive to excitation energies. To help explain this idea, Figure 1.1 shows an example Franck-Condon Weighted DOS used in the calculations detailed later in this thesis, plotted by the driving force. Even a 0.5 eV difference in driving force can change the TTET rate by a factor of five.

Another unresolved issue in TTET calculations is the choice of geometry. Some studies use ground-state optimized geometries [10], and others triplet-state optimized geometries [11], neither with any justification for their choice. The electronic coupling and excitation energies depend strongly on the geometry used, making them very important for accurate TTET calculations. With current computational methods it is very difficult to optimize triplet-state geometries accurately, and triplet excitation calculations are very sensitive to these geometries.

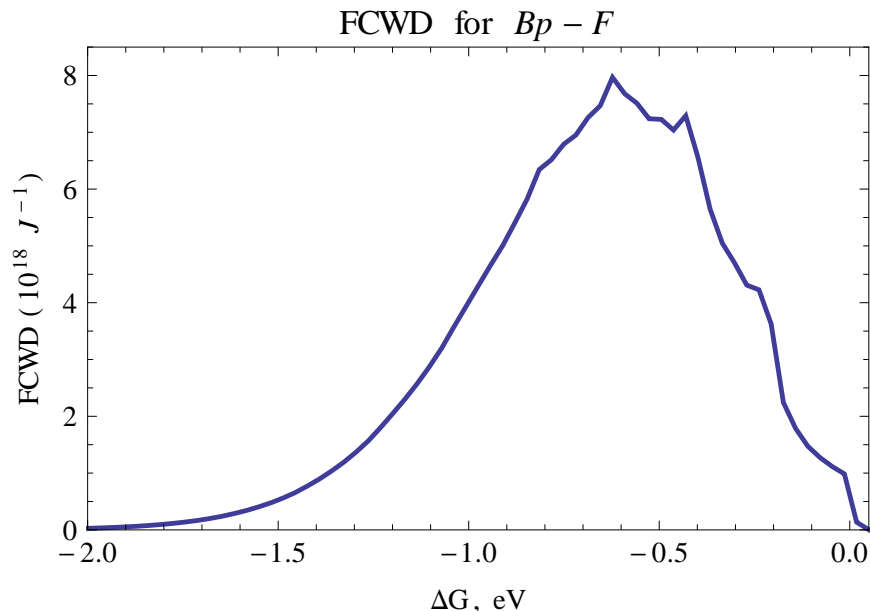


Figure 1.1: FCWD for the  $Bp \rightarrow F$  Transition

This thesis will discuss many of the methods and calculations involved in predicting TTET rates, and their accuracy and sources of error. The discussion sections will suggest improvements to the methods used in literature, which aim to best predict accurate TTET rates while minimizing empirical influence.

### 1.1 The $Bp$ - $F$ - $Nap$ Molecule

This thesis investigates TTET on the benzophenone-fluorene-naphthalene molecule ( $Bp$ - $F$ - $Nap$ ), shown in Figure 1.2. The  $Bp$ - $F$ - $Nap$  molecule is uniquely capable of TTET for two reasons: 1) on  $Bp$ , the donor molecule, nearly all excitations quickly transition into the lowest triplet state via intersystem crossing [3], and 2) there is a “downhill” energy gradient along  $donor \rightarrow bridge \rightarrow acceptor$  [10]. Reason 2 simply indicates that the exciton will likely move along the path  $donor \rightarrow bridge \rightarrow acceptor$ . Reason 1 ensures that the donor will only produce triplet states, which is a very peculiar quality of  $Bp$ .

The  $Bp$  molecule has been an object of curiosity for the better part of this century. Of particular interest is the lowest triplet state of  $Bp$ , which has been the subject of numerous

experimental studies [12–14]. Optical excitations in *Bp* quickly decay (within picoseconds) into the lowest triplet state, which is relatively stable. This rapid intersystem crossing is very useful for generating triplet excitons, but its cause is not very well understood. The physical effects that give rise to the strange behavior of *Bp* have also caused problems in electronic calculations of this molecule, as discussed in Section 3.2.

The rapid intersystem crossing of *Bp* has been studied extensively, yet it is not completely understood. This strange property, while useful for triplet generation, is likely the cause of many problems encountered by excited-state calculations.

The following sections discuss one experimental and one computational study of TTET rates on the *Bp-F-Nap* molecule, which are used for comparison throughout this thesis.

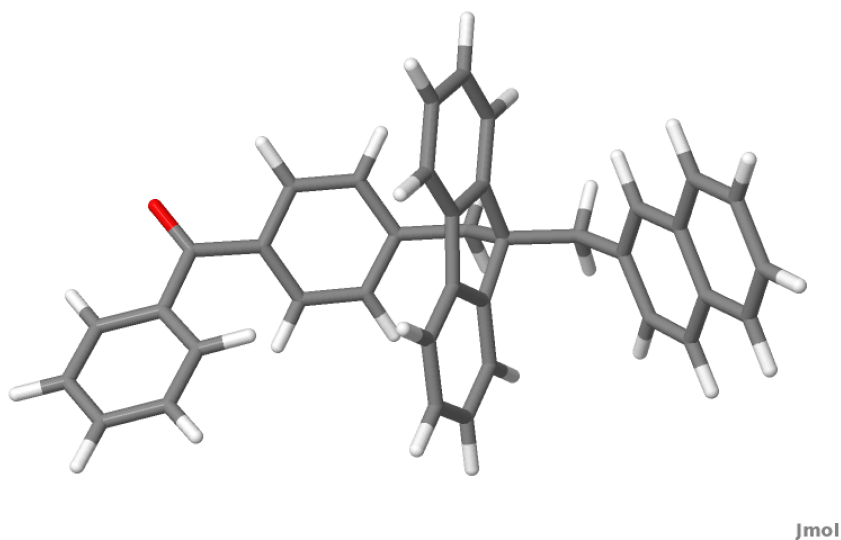


Figure 1.2: The *Bp-F-Nap* molecule

## 1.2 Experimental Benchmark

The *Bp-F-Nap* system was studied experimentally by Vura-Weis et al. in [10]. Both *sequential hopping* and *superexchange* (or tunneling) rates were measured, using transient absorption spectra. These experimental hopping rates will be compared to the computational results presented in this thesis; this experimental study is just one example of many such

measurements of TTET rates available for comparison with computational models.

### 1.3 Computational Benchmark

Si et al. published a computational study of TTET on *Bp-F-Nap*, using a diabatic-state approach [11]. Their rates were slightly higher than those measured by Vura-Weis et al., but still very close for an ab initio study. However, the methods used by Si et al. required some empirical knowledge of the system, and some unexplained approximations, making them difficult to use in predictive studies. The rates calculated in [11] will be compared to the results presented in this thesis, and suggestions will be made to improve these calculations. Specifically, the approximations made in [11] will be discussed, and suggestions will be proposed to make such calculations less empirical.

One important result presented by Si et al. is the comparison of superexchange to sequential hopping. They find that superexchange coupling between the *Bp* donor and the *Nap* acceptor is two orders of magnitude smaller than their direct electronic coupling, making the superexchange process much slower than the sequential hopping process. For this reason, superexchange rates are not calculated in this thesis.

Chapter 2 will discuss the proposed expression for the TTET rate, and the many physical parameters which constitute it. Calculations of these physical parameters are presented and discussed in Chapters 3, 4, and 5. The final rate calculations are discussed in Chapter 6.

## CHAPTER 2

### THEORY

This thesis seeks to elucidate the computational methodology associated with the calculation of TRET rates between small organic molecules. Experiments indicate that this type of hopping occurs in the incoherent regime [15]; this is confirmed by the comparison of reorganization and electronic coupling energies in Chapters 3 and 4. In the incoherent regime, we can use Fermi’s Golden Rule (FGR)[9] for the transport rate:

$$k_{i \rightarrow f} = \frac{2\pi}{\hbar} |V_{if}|^2 \rho, \quad (2.1)$$

where  $V_{if} = \langle f | W | i \rangle$  is the perturbation term due to  $W$  between the initial ( $|i\rangle$ ) and final ( $|f\rangle$ ) states, and  $\rho$  is the density of states. The FGR is based on a first-order perturbation of the system Hamiltonian to calculate the projection of  $|i\rangle$  onto  $|f\rangle$ . These states account for both electronic and phonon states. However because these transitions occur in the incoherent regime, we can make the *Condon approximation* [9], that the electronic interaction does not depend on the initial and final vibrational states of the system:

$$\langle \phi_f; \chi_f | W | \phi_i; \chi_i \rangle = \langle \phi_f | W | \phi_i \rangle \times \langle \chi_f | \chi_i \rangle, \quad (2.2)$$

where  $|\phi\rangle$  is an electronic state, and  $|\chi\rangle$  is a vibrational state. This approximation also implies that the electronic states are *adiabatic* – that is, the electronic orbitals are independent of the vibrational coordinates. This is an important distinction; expressions for the parameters  $\rho$  and  $V_{if}$  – which determine the rate in equation 2.1 – depend on whether adiabatic or diabatic states are used. The difference between these states is discussed in the following section.

#### 2.1 Diabatic and Adiabatic States

We seek to calculate the rate at which an exciton hops from one moiety to another, but the initial and final states associated with such an event are difficult to ascertain. They are

necessarily not associated with global equilibrium states of the system but, rather, with local equilibria. Excitons can tunnel out of these states with or without vibrational assistance, and it is such rates that we are trying to quantify.

The difference between the global and local equilibria can be described in terms of *adiabatic* and *diabatic* processes, respectively. In a diabatic process, electrons react to local dynamics of the nuclei, while electrons have time to react to the global nuclei environment in adiabatic processes. From a thermodynamics perspective, an adiabatic process is one in which there is no transfer of heat. On the molecular scale, this corresponds to a process which does not involve energy transferred to or from the phonon states of the system. Thus, an adiabatic process assumes that the nuclei can be treated as static, and that the electrons react very quickly to nuclear displacements so that the electronic structure is always an eigenstate that parametrically depends on atomic positions. On the other hand, diabatic processes assume that the nuclei and electron dynamics proceed at comparable rates, and their dynamic interactions must be considered. It is often helpful to ask if a given system is in an electronic eigenstate for the prescribed atomic positions. If so, it is an adiabatic state.

This distinction can also be understood through the Born-Oppenheimer approximation [16] in which the electronic and vibrational components of a wave function are assumed to be separable. This amounts to an adiabatic assumption. For further illustration, Figure 2.1 shows potential energy surfaces (PESs) for diabatic and adiabatic states, and how they relate to the hopping parameters in Equation 2.1; these parameters are discussed in the following sections.

Bringing these concepts home to the TTET investigation, an electronic structure calculation on the entire *Bp-F-Nap* assembly will yield adiabatic states that are not relevant in hopping dynamics because the initial and final states associated with an exciton hop are necessarily electronic states that are out of equilibrium relative to the atomic positions—i.e. they are not eigenstates. This is a computationally difficult position to be in, but there are several approaches that are used to estimate the (diabatic) initial and final states. One

approach is to simply obtain the (adiabatic) eigenstates of each moiety separately. Initial and final excitonic states can then be constructed out of these isolated eigenstates, and such composite states are treated as diabatic states for the entire assembly – i.e. as local equilibrium states. Another approach is to try to confine constrained excitonic orbitals to one moiety or another, again to approximate local equilibria. These methods are discussed in detail subsequently.

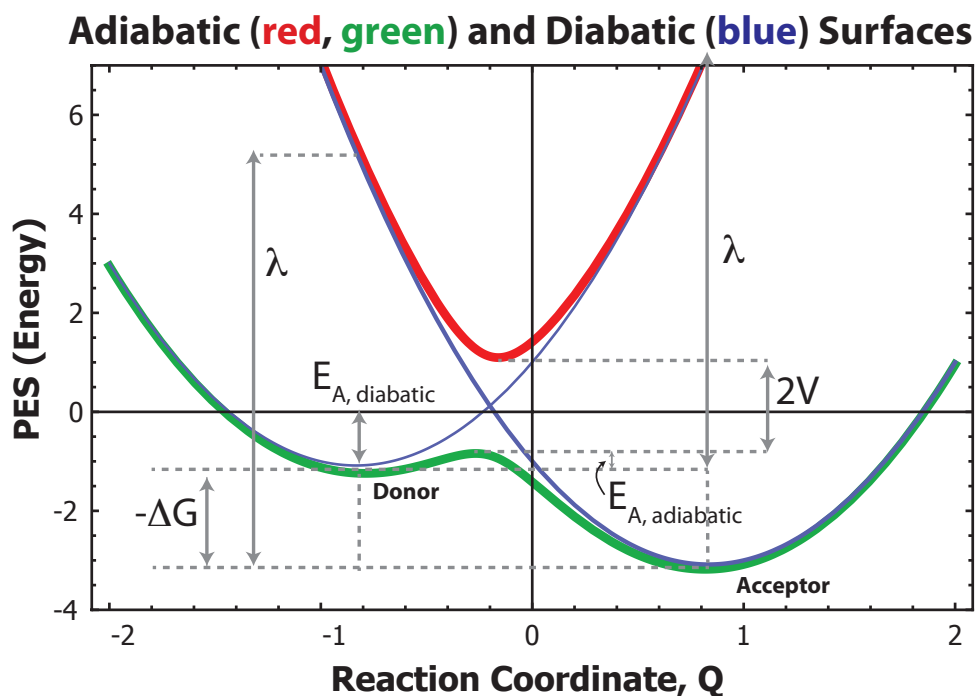


Figure 2.1: Diabatic and adiabatic PESs;  $\lambda$  is the reorganization energy,  $V$  is the electronic coupling, and  $\Delta G$  is the driving force

**Notation:** For simplicity, we will use superscripts to indicate the presence of a triplet state, and the notation (*geometry*||*occupation*) to describe the geometry and electronic occupation used. For example:

### Diabatic States

- $(D^3 - A || D - A)$ : The donor-acceptor dimer; optimized with a triplet on the donor; in the ground electronic state.
- $(D - B - A || D - B^3 - A)$ : The donor-bridge-acceptor molecule; optimized in the ground electronic state; with a triplet confined on the bridge.

### Adiabatic States

- $(A || A^3)$ : The acceptor molecule; optimized in the ground state; in the triplet electronic state.

## 2.2 Density of States

The density of states  $\rho$  represents the number of available transitions from initial to final states in equation 2.1. Because the *Bp-F-Nap* system is a strongly confined system its energy levels are very discrete, so the only significant contribution to  $\rho$  that we need to consider is exciton-phonon interaction.

**Exciton-Phonon Interaction:** When a molecule transitions into an excited electronic state, its geometry relaxes as well – using the above notation, this is the transition from  $(X || X^3)$  to  $(X^3 || X^3)$ . Letting  $\Delta\vec{Q}$  be the total change in geometry,

$$\Delta\vec{Q} = \text{geom}(X^3) - \text{geom}(X),$$

then in the harmonic approximation, the individual contribution from each phonon mode  $\hat{e}_i$  is [17]

$$\Delta\vec{Q}_i = \Delta\vec{Q} \cdot \hat{e}_i.$$

Using these  $\Delta\vec{Q}_i$  we can define the mode-specific reorganization energy as

$$\lambda_i = \frac{1}{2}\omega_i\Delta Q_i^2, \tag{2.3}$$

where  $\omega_i$  is the frequency of the  $i^{th}$  mode. We can then define the *Huang-Rhys Factor* [9] of the  $i^{th}$  mode as

$$S_i = \lambda_i / \hbar \omega_i. \quad (2.4)$$

### 2.2.1 FCWD

As shown in equation 2.2, adiabatic electronic states neglect exciton-phonon interactions. Such interactions are important for these rate calculations, even in the incoherent regime [18]; for this reason we will incorporate exciton-phonon interactions using the Franck-Condon weighted density of states (FCWD) [9, 17]. The exciton-phonon interaction density of states is simply a sum of delta-functions, one for each phonon mode. These delta functions can be expressed a time-integral of of a complex exponent, which results in the expression for the FCWD:

$$\rho_{FCWD} = \frac{1}{2\pi\hbar} \int_{-\infty}^{+\infty} dt \exp \left\{ i \frac{\Delta E}{\hbar} t - \sum_j S_j [(2n_j + 1) - n_j e^{-i\omega_j t} - (n_j + 1) e^{i\omega_j t}] \right\}, \quad (2.5)$$

where  $S_j$  and  $\omega_j$  are the Huang-Rhys factors and frequencies of the  $j^{th}$  phonon mode, and  $\Delta E$  is the change in optical gap during the process.  $n_j$  is the phonon occupation number,

$$n_j = \frac{1}{\exp(\hbar\omega_j/k_B T) - 1}.$$

Because the FCWD uses adiabatic states, yet includes exciton-phonon interactions, it is termed a *nonadiabatic* method. Lorentzian and Gaussian distributions are typically used to account for various broadenings of  $\rho$ . Thermal broadening (due to exciton-phonon interactions) and natural broadening (due to the uncertainty principle) are often Lorentzian, while other contributions such as inhomogeneous broadening and Doppler broadening are Gaussian [19]. As expected, the FCWD resembles a Gaussian and Lorentzian distribution, as shown in Figure 2.2. This FCWD was generated for the  $Bp \rightarrow F$  transition, and it is plotted along with both Gaussian and Lorentzian fits.

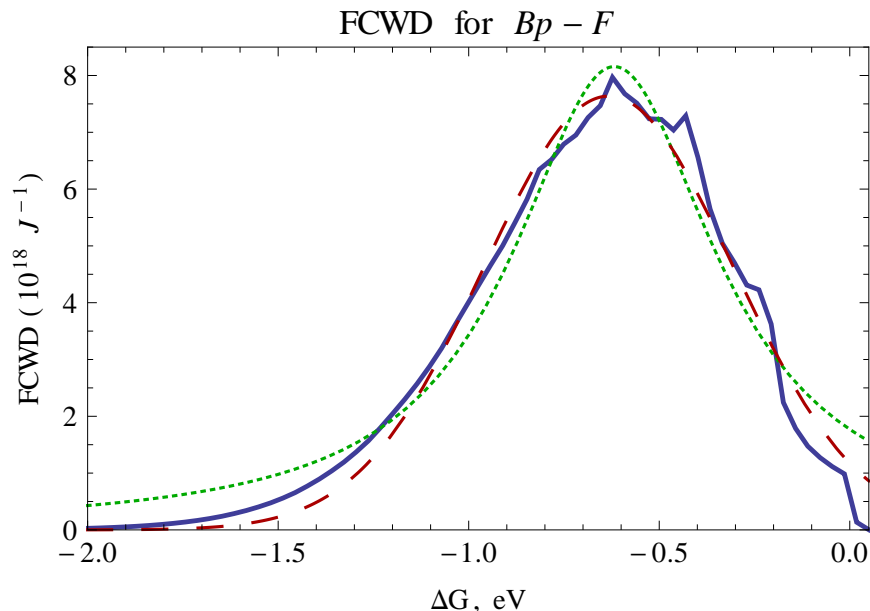


Figure 2.2: FCWD for the  $Bp \rightarrow F$  transition (solid blue), with Gaussian (red dashes) and Lorentzian (green dots) fits

### 2.3 Electronic Coupling

Coulomb interactions, which typically dominate Förster resonant energy transfer, are not relevant in triplet-triplet energy transport because the associated orbitals involved in Coulomb integrals have orthogonal spins. This means that the simplest estimate for electronic coupling (the calculation of Coulomb integrals) cannot be used in the present setting. However, a related contribution to electronic coupling comes from Dexter interactions associated with triplet-triplet coupling. This can be estimated with integrals that capture exchange interactions [20]. However recent computational studies have shown that Dexter coupling is insufficient to accurately predict TTET rates [4, 5]. A more comprehensive method is needed. Two such methods are studied in this thesis – Hartree-Fock coupling and the fragment-spin-difference method.

### 2.3.1 Hartree-Fock Coupling – Diabatic States

The biggest challenge in calculating electronic coupling is finding the correct initial and final states to use. Voorhis and Yeganeh proposed a method of calculating these states using constrained-DFT (CDFT) [4], which assumes that the physically correct initial and final (diabatic) states have the triplet spin density completely confined to the donor and acceptor molecules, respectively. CDFT is used to confine the spin density, and the spin constraints are used to optimize the *donor-acceptor* dimer into the appropriate geometry.

The electronic coupling is then the off-diagonal electronic Hamiltonian term between the initial and final diabatic states,

$$V_{if} = \langle D - A^3 | H_{el} | D^3 - A \rangle.$$

Because these states calculated within CDFT are not guaranteed to be orthogonal, the Löwdin method is used to find orthogonal eigenstates; the off-diagonal Hamiltonian matrix element for these orthogonalized states is then used in the FGR:

$$V_{HF} = \frac{H_{DA} - S_{DA}(\epsilon_d - \epsilon_a)/2}{1 - S_{DA}^2},$$

where  $H_{if}$  and  $S_{if}$  are the coupling and overlap between the donor and acceptor CDFT-calculated diabatic states, and  $\epsilon_d$  and  $\epsilon_a$  are the CDFT-diabatic state energies. The Hamiltonian and overlap matrix elements  $H_{DA}$  and  $S_{DA}$  can be evaluated using the Hartree-Fock Hamiltonian and orbitals, which is why this method is referred to as Hartree-Fock (HF) coupling.

Because HF coupling uses CDFT-diabatic states, it requires a computational package that can perform spin-restricted CDFT (such as Q-Chem [21]). Si et al. successfully employed this coupling method in [11], as discussed in Section 4.

## 2.4 Fragment Spin Difference – Adiabatic States

Because diabatic states are often difficult to calculate, it is easier to first find adiabatic states, and then use a superposition of these to generate diabatic states. Such a method was proposed by You and Hsu [5] – the fragment spin difference (FSD) method. FSD coupling is based on the fragment *charge* difference method, which was developed by Voityuk and Rösch [22] for electron transport. The FSD method is best understood by first discussing FCD, which begins by defining two adiabatic states:

$$\begin{aligned}\psi_1 &= c_{D1}\phi_D + c_{A1}\phi_A \\ \psi_2 &= c_{D2}\phi_D + c_{A2}\phi_A,\end{aligned}\tag{2.6}$$

where  $\phi_D$  and  $\phi_A$  are diabatic orbitals localized on the donor and acceptor, respectively. An orthogonal transformation is used on  $\psi_1$  and  $\psi_2$  to obtain two new states,  $\tilde{\psi}_D$  and  $\tilde{\psi}_A$ :

$$\begin{pmatrix} \tilde{\psi}_D \\ \tilde{\psi}_A \end{pmatrix} = \begin{pmatrix} \cos(\theta) & -\sin(\theta) \\ \sin(\theta) & \cos(\theta) \end{pmatrix} \begin{pmatrix} \psi_1 \\ \psi_2 \end{pmatrix}.\tag{2.7}$$

In the state  $\tilde{\psi}_D$ , the charge on the donor is

$$\begin{aligned}q_D(\tilde{\psi}_D) &= (c_{D1}\cos(\theta) - c_{D2}\sin(\theta))^2 \\ &= q_1(D)\cos^2(\theta) + q_2(D)\sin^2(\theta) - q_{12}(D)\sin^2(2\theta),\end{aligned}\tag{2.8}$$

and similarly for the state  $\tilde{\psi}_A$ , the charge on the acceptor is

$$\begin{aligned}q_A(\tilde{\psi}_A) &= (c_{A1}\cos(\theta) + c_{A2}\sin(\theta))^2 \\ &= q_1(A)\cos^2(\theta) + q_2(A)\sin^2(\theta) + q_{12}(A)\sin^2(2\theta),\end{aligned}\tag{2.9}$$

where the following substitutions have been made:

$$\begin{aligned}q_{ij}(D) &= c_{Di}c_{Dj} \\ q_{ij}(A) &= c_{Ai}c_{Aj}\end{aligned}\tag{2.10}$$

$$\Delta q_{ij} = q_{ij}(D) - q_{ij}(A).$$

In order to find the *maximum charge difference* between these two states, we must find the rotation angle  $\theta$  that maximizes the sum of charges on the donor and acceptor,  $q_{tot} = q_A(\tilde{\psi}_A) + q_D(\tilde{\psi}_D)$ . This is easily done by setting  $\frac{dq}{d\theta} = 0$ , which yields

$$\tan(2\theta) = \frac{2\Delta q_{12}}{\Delta q_{22} - \Delta q_{11}}, \quad (2.11)$$

By using equations 2.7 and 2.11 it is easily shown that the coupling is

$$\begin{aligned} V_{12}^{\text{FCD}} &= \langle \tilde{\psi}_D | H | \tilde{\psi}_A \rangle \\ &= \frac{(E_2 - E_1)|\Delta q_{12}|}{\sqrt{(\Delta q_{11} - \Delta q_{22})^2 + 4\Delta q_{12}^2}}, \end{aligned} \quad (2.12)$$

where  $E_i$  is the energy of the  $i^{\text{th}}$  electronic state.

FSD coupling adapts this method to TTET by changing the charge difference terms  $\Delta q_{ij}$  to *spin difference* terms, defined as

$$\begin{aligned} s_{ij}(\mathbf{r}) &= \rho_{ij}^\alpha(\mathbf{r}) - \rho_{ij}^\beta(\mathbf{r}) \\ \Delta s_{ij} &= \int_{\mathbf{r} \in D} s_{ij}(\mathbf{r}) - \int_{\mathbf{r} \in A} s_{ij}(\mathbf{r}), \end{aligned} \quad (2.13)$$

where  $i$  and  $j$  are excited (adiabatic) states of the system; and for  $\rho_{ij}$ ,  $i = j$  indicates the spin density for the  $i^{\text{th}}$  excited state for, and  $i \neq j$  indicates the transition spin density between the  $i^{\text{th}}$  and  $j^{\text{th}}$  states. The integrals in equation 2.13 are over the spatial regions of the donor ( $D$ ) and acceptor ( $A$ ), which must be specified by the investigator. The FSD coupling is then

$$V_{12}^{\text{FSD}} = \frac{(E_2 - E_1)|\Delta s_{12}|}{\sqrt{(\Delta s_{11} - \Delta s_{22})^2 + 4\Delta s_{12}^2}}, \quad (2.14)$$

where  $E_i$  is the energy of the  $i^{\text{th}}$  excited (adiabatic) state. Similarly to the fragment charge difference method, FSD maximizes the *spin difference* between the donor and acceptor excitations.

The fundamental difference between HF coupling and FSD coupling is the order of operations. Both methods assume that the physically correct (diabatic) initial and final states

have the triplet spin density localized on the donor and acceptor molecules, respectively. HF coupling achieves this end by calculating these diabatic states from the start; on the other hand, FSD coupling first calculates adiabatic states (eigenvalues of the *donor-acceptor* system), and then satisfies the spin restriction using a superposition of the adiabatic states.

## 2.5 Driving Force $\Delta G$

The driving force is defined as the change in free energy during the hopping process [23]:

$$\begin{aligned} \Delta G = & E(D^3 - A||D - A^3) - E(D - A^3||D - A^3) \\ & + E_{opt}(D^3 - A||D^3 - A) - E_{opt}(D - A^3||D - A^3), \end{aligned} \quad (2.15)$$

where  $E()$  indicates a total system energy, and  $E_{opt}()$  is the optical gap. As discussed earlier, the initial and final states are *diabatic*, because they are not eigenstates of the *donor-acceptor* system. The driving force can be separated into the *reorganization energy*  $\lambda$ :

$$\lambda = E(D^3 - A||D - A^3) - E(D - A^3||D - A^3),$$

and the difference in optical gap  $\Delta E$ :

$$\Delta E = opt(D^3 - A||D^3 - A) - opt(D - A^3||D - A^3).$$

$\Delta E$  accounts for changes in the excitation energy during hopping, while  $\lambda$  accounts for geometric relaxation during hopping. In this thesis we use the FCWD, which accounts for  $\lambda$  by calculating exciton-phonon interactions; for this reason  $\lambda$  will not be used explicitly in equation 2.1. Instead,  $\lambda$  will be compared to the sum of all modal reorganization energies to check the vibrational analysis, as discussed below.

### 2.5.1 Reorganization Energy

Without approximation, the reorganization energy for TTET is

$$\lambda_{direct} = E(D^3 - A||D - A^3) - E(D - A^3||D - A^3).$$

Assuming that the interaction between donor and acceptor geometries is small, we can use adiabatic states instead of diabatic – that is, geometries optimized into the eigenstate of the individual donor and acceptor molecules (this is sometimes called the four-point method) [11]:

$$\lambda_{4\text{-point}} = E(D^3||D) - E(D||D) + E(A||A^3) - E(A^3||A^3).$$

$\lambda$  can also be expressed through the vibronic structure, as a sum of the mode-specific reorganization energies:

$$\lambda_{vib} = \sum_i \lambda_i.$$

$\lambda_{vib}$  is not recommended to estimate reorganization energy; rather it should be compared to  $\lambda_{direct}$  or  $\lambda_{4\text{-point}}$  to check the validity of a calculated vibronic structure.

## 2.6 Ground State Electronic Structure Calculations

All of the physical properties above are estimated using density functional theory (DFT), an ab initio ground state method. The core principles of DFT are the Hohenberg-Kohn theorems, which state that for an  $N$ -electron system in an external potential<sup>1</sup>:

1. The external potential – and therefore the total system energy – is uniquely determined by a functional of the  $N$ -electron density.
2. The minimum of this functional is the *exact* ground-state energy, and the corresponding  $N$ -electron density is the *exact* ground-state density.

The expression for this  $N$ -electron density is based on the Kohn-Sham equation for a system of non-interacting electrons [24]:

---

<sup>1</sup>As these theorems indicate, DFT is only a ground-state theory – all excited-state DFT calculations should be used with caution.

$$\left(-\frac{\hbar^2}{2m}\nabla^2 + V_{eff}(\mathbf{r})\right)\phi_i(\mathbf{r}) = \epsilon_i\phi_i(\mathbf{r}),$$

where the  $\epsilon_i$  are the energies of the Kohn-Sham orbitals  $\phi_i$ . The electron density for an  $N$ -particle system is then

$$\rho(\mathbf{r}) = \sum_i^N |\phi_i(\mathbf{r})|^2.$$

The *Kohn-Sham potential*  $V_{eff}$  is [25]

$$V_{eff}(\mathbf{r}) = V_{ext}(\mathbf{r}) + q_e^2 \int d\mathbf{r}' \frac{\rho(\mathbf{r}')}{|\mathbf{r} - \mathbf{r}'|} + \frac{\delta E_{xc}[\rho]}{\delta \rho(\mathbf{r})},$$

where  $V_{ext}$  is the external potential (in this case, only due to nuclei), the second term is the electrostatic potential, and the third term is the *exchange-correlation potential*  $V_{xc}$ . These are called the Kohn-Sham equations, which must be solved self-consistently. There is only one term in this equation that cannot be solved for exactly – the exchange-correlation functional  $E_{xc}$ ; the following section discusses various approximations for  $E_{xc}$ .

### 2.6.1 Exchange-Correlation Functionals

For all systems (except for the electron gas),  $E_{xc}$  is not known; for this reason we must choose an approximation method [9].

**Hartree-Fock:** In the Hartree-Fock method (HF), the exchange interaction is calculated exactly while the electron correlation is neglected. The Hartree-Fock “exact” exchange functional is

$$E_x^{HF} = \frac{1}{2} \sum_{i,j} \int \int d^3\mathbf{r}_1 d^3\mathbf{r}_2 \psi_i^*(\mathbf{r}_1)\psi_j^*(\mathbf{r}_1) \frac{1}{r_{12}} \psi_i(\mathbf{r}_2)\psi_j(\mathbf{r}_2)$$

HF exchange is often included in the hybrid functionals discussed below.

**Local Density Approximation:** The most commonly used exchange-correlation functional is the Local Density Approximation (LDA), which assumes that  $E_{xc}$  only depends *locally* on  $\rho$ :

$$E_{xc}^{LDA} = \int d^3\mathbf{r} \epsilon_{xc}(\rho(\mathbf{r}))\rho(\mathbf{r}).$$

There are many analytic forms of  $\epsilon_{xc}$  that may be used. Most calculations in this thesis used an  $E_{xc}$  proposed by Perdew and Wang [26], commonly referred to as PWC.

**Generalized Gradient Approximation:** An improvement to LDA is the Generalized Gradient Approximation (GGA), which also considers the gradient of  $\rho$ :

$$E_{xc}^{GGA} = \int d^3\mathbf{r} \epsilon_{xc}(\rho(\mathbf{r}), \Delta\rho(\mathbf{r}))\rho(\mathbf{r}).$$

As for LDA, there are many GGA forms of  $E_{xc}$ ; many calculations in this thesis use a functional proposed by Perdew, Burke, and Ernzerhof [27], commonly referred to as PBE.

**Hybrid Functionals:** A further correction to LDA and GGA is the hybrid functional, which include LDA and GGA exchange correlation, as well as Hartree-Fock exchange. The only hybrid functional used in this thesis is that proposed by Lee, Yang, and Parr [28], commonly referred to as B3LYP.

### 2.6.2 Excited State Electronic Structure Calculations

Excited state calculations are more difficult and complicated than ground state calculations. There are many excited state theories, and most of them are improvements of DFT.

**DFT HOMO-LUMO Gap:** The most basic approximation of optical gap used is the DFT HOMO-LUMO energy gap – that is, the difference between the highest occupied molecular orbital (HOMO) and the lowest unoccupied molecular orbital (LUMO), of a DFT calculation. To calculate a triplet HOMO-LUMO gap, we restrict the spins of the two highest Kohn-

Kohn-Sham orbitals to be parallel. Because DFT is strictly a ground-state theory, this is a very rough estimation of optical gap; to improve it, we can include quasi-particle effects using the GW approximation.

**Quasi-Particle Effects and GW:** Hedin proposed a correction to the excited-state DFT energies using single-particle Green's functions [29]. He applies a perturbation to the excited-state DFT energies (LUMO and above), based on the screened Coulomb interaction and the polarizability; this correction is called the GW approximation. The GW correction estimates *quasi-particle energies* – that is, the energy required to add or remove an electron from the system [7]. Figure 2.3 shows some example systems for which GW predicts the experimental optical gap better than DFT (LDA) [30]. Quasi-particle energies correspond to the energy required to add or remove an electron from a system – making them useful for charged systems, but not ideal for neutral excitations.

For this reason GW quasi-particle calculations are not reported in this thesis, although they are just used to calculate BSE energies.

**GW+BSE:** While GW quasi-particle energies are useful for investigating charged systems, they do not account for neutral excitations such as those involved in TTET. Instead the Bethe-Salpeter equation is used, which uses two-particle (electron-hole) Green's function to include excitonic effects [7]. It has been shown that, for confined systems and small molecules, the BSE method can more accurately calculate excitation energies [7, 31].

**TDDFT:** Time-Dependent Density Functional Theory (TDDFT) uses the same theoretical framework as DFT – Kohn-Sham orbitals – only TDDFT uses a time-dependent density and time-dependent potential. This method is based on the Runge-Gross theorem [6] – the time-dependent counterpart to the Hohenberg-Kohn theorem discussed in Section 2.6. Excitations within TDDFT are calculated using all available states, not just the HOMO and LUMO as the DFT gap does. This provides a significant improvement to optical gap

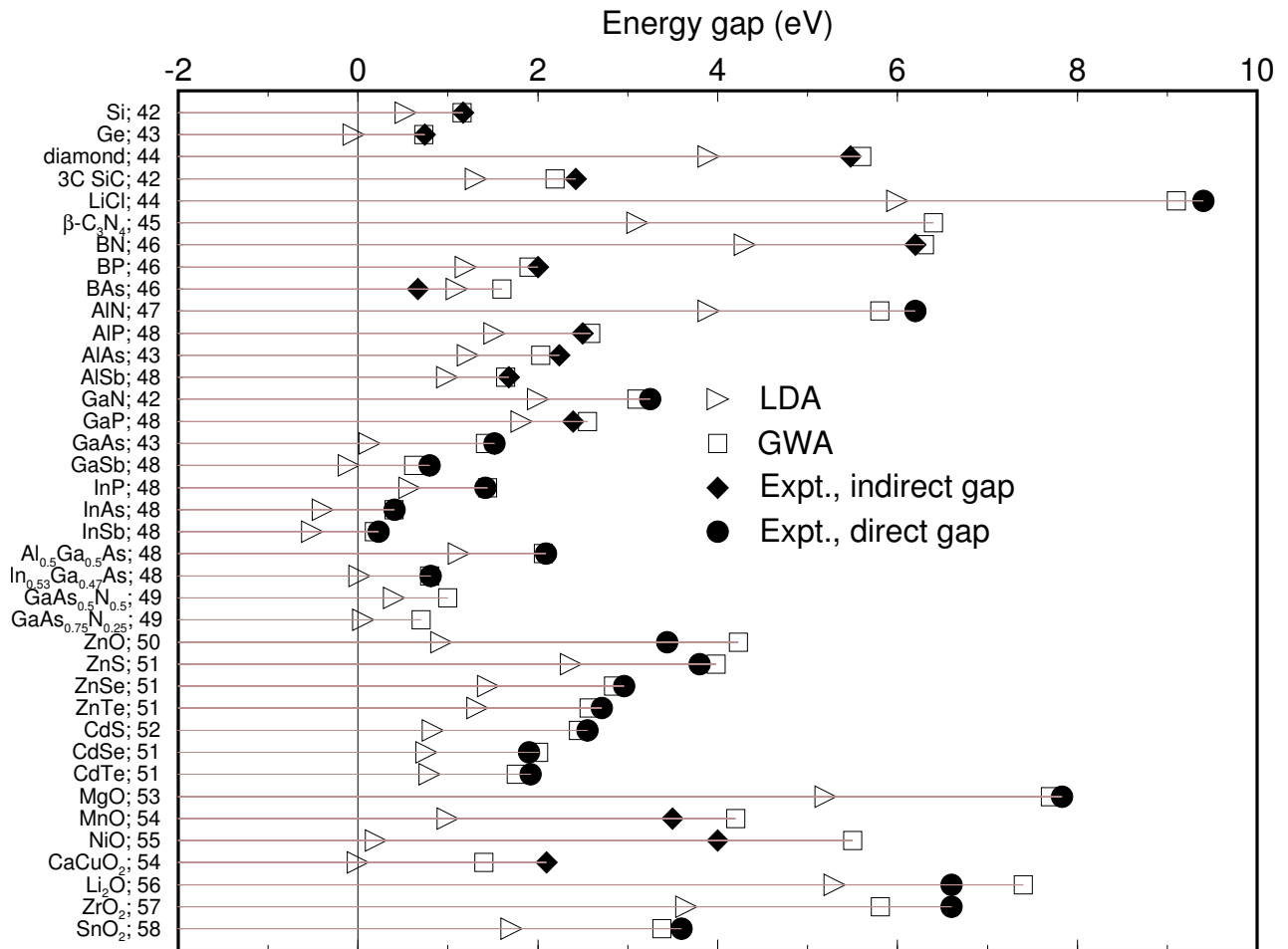


Figure 2.3: Comparison of GW and DFT (LDA) optical gaps [30]

calculations.

**CIS:** Configuration Interaction Singles (CIS) is identical to TDDFT, save for two differences 1) CIS uses the Hartree-Fock exchange instead of a DFT exchange-correlation functional, and 2) CIS makes the Tamm-Dancoff approximation [32] – which only considers single electron-hole excitations [33]. The CIS method can be extended to include single and double excitations (CISD), triples (CISDT), and so on.

## CHAPTER 3

### COMPUTATIONAL IMPLEMENTATION: OPTICAL GAP

This chapter discusses calculations of optical gap using DFT, GW+BSE, and TDDFT. Two sets of geometries were used in these calculations. Each molecule was optimized – *Bp-me*<sup>2</sup>, *F-me*, and *Nap-me* – into a ground-state geometry, and a triplet-excited state geometry. The ground-state optimizations used spin-restricted calculations, while the triplet-state optimizations used spin-unrestricted calculations with the total spin set to 2. Both PBE and LDA XC-functionals were used; all optimization were done in DMol 3 [34].

**DFT HOMO-LUMO Gap:** All DFT HOMO-LUMO gaps were calculated using DMol. As expected the DFT HOMO-LUMO gap calculations (see Table 3.1) are not very close to experiment, but they did indicate a downhill driving force, suggesting that hopping from *Bp* to *F* to *Nap* is possible. The choice of exchange-correlation functional also appears to have little effect on DFT. The HOMO levels for both PBE and LDA are within 0.1 eV of each other, while the LUMO energies are about 0.3 eV higher with LDA.

**GW+BSE:** All GW+BSE gaps were calculated using Parsec & RGWBS [7]. BSE calculations (see Table 3.2) were much closer to experiment than any other method, for fluorene and naphthalene. However the BSE results for benzophenone were consistently about 0.5 eV below experimental values. Although he did not consider BSE calculation, Si et al. also encountered a problem in estimating the optical gap of benzophenone, and this is discussed in Section 3.2.

**TDDFT:** All TDDFT gaps were calculated using Q-Chem [21], and some calculations used the SM8 [35] solvation model with H<sub>2</sub>O. TDDFT calculations are listed in Table 3.3 and

---

<sup>2</sup>The *-me* indicates that a methyl group is attached where the molecule would connect to its neighbor.

Table 3.1: Triplet DFT HOMO-LUMO gaps (eV)

<i>molecule</i>		<b>LDA</b>		<b>PBE</b>		<b>Lit.[10]</b>
		Ground	Triplet	Ground	Triplet	
<i>Bp-me</i>	HOMO	-6.27	-6.08	-5.93	-5.73	
	LUMO	-3.27	-3.53	-3.15	-3.46	
	<b>gap</b>	<b>3.00</b>	<b>2.55</b>	<b>2.78</b>	<b>2.27</b>	<b>3.11</b>
<i>F-me</i>	HOMO	-5.50	-5.15	-5.15	-4.78	
	LUMO	-2.34	-2.66	-2.25	-2.61	
	<b>gap</b>	<b>3.16</b>	<b>2.48</b>	<b>2.90</b>	<b>2.17</b>	<b>2.87</b>
<i>Nap-me</i>	HOMO	-5.31	-4.99	-4.96	-4.61	
	LUMO	-2.45	-2.85	-2.40	-2.81	
	<b>gap</b>	<b>2.86</b>	<b>2.14</b>	<b>2.56</b>	<b>1.80</b>	<b>2.60</b>

Table 3.2: Triplet BSE energies, for geometries optimized into the LDA and PBE ground and triplet states (eV)

<i>molecule</i>	<b>LDA Geometries</b>		<b>PBE Geometries</b>		<b>Lit. [10]</b>
	Ground	Triplet	Ground	Triplet	
<i>Bp-me</i>	2.43	1.81	2.36	1.69	<b>3.11</b>
<i>F-me</i>	2.74	2.02	2.66	1.91	<b>2.87</b>
<i>Nap-me</i>	2.45	1.71	2.36	1.60	<b>2.60</b>

Table 3.4. Both the PBE and B3LYP XC functionals were used as noted, and all calculations use the 6-31+G\* basis functions. As discussed in Chapter 4, the 6-31+G\* basis is consistent with other long-range and numerical basis sets, so it is appropriate for use in the *Bp-F-Nap* system.

While the TDDFT calculations were not as close to experiment as BSE, the Q-Chem software allowed for the inclusion solvent effects and different functionals. As found in the DFT and GW+BSE calculations, excitation energies calculated using triplet geometries severely over-estimate the Stokes shift.

Table 3.3: Triplet TDDFT energies, PBE-ground-state geometry (eV)

<i>molecule</i>	No Solvent		In H2O		Lit. [10]
	PBE	B3LYP	PBE	B3LYP	
<i>Bp-me</i>	2.60	3.01	2.90	3.27	<b>3.11</b>
<i>F-me</i>	3.12	3.31	3.13	3.32	<b>2.87</b>
<i>Nap-me</i>	2.84	3.02	2.84	3.01	<b>2.60</b>

Table 3.4: Triplet TDDFT energies, PBE-excited-state geometry (eV)

<i>molecule</i>	No Solvent		In H2O		Lit. [10]
	PBE	B3LYP	PBE	B3LYP	
<i>Bp-me</i>	1.95	2.33	N/A	N/A	<b>3.11</b>
<i>F-me</i>	2.44	2.56	2.45	2.57	<b>2.87</b>
<i>Nap-me</i>	2.13	2.24	2.13	2.24	<b>2.60</b>

**CIS:** CIS gaps were calculated using Q-Chem; these results are listed in table Table 3.5, and they are converged in the number of single excitations used<sup>3</sup>. These calculations are by far the closest to experimental values.

<sup>3</sup>These calculations are identical to the TDDFT calculations discussed above, only the Hartree-Fock exchange is used instead of an exchange-correlation functional like PBE or B3LYP.

Table 3.5: Triplet CIS energies, for geometries optimized into the PBE ground and triplet states (eV)

<i>molecule</i>	Ground Geometry	Triplet Geometry	Lit. [10]
<i>Bp-me</i>	3.10	2.64	<b>3.11</b>
<i>F-me</i>	2.84	2.12	<b>2.87</b>
<i>Nap-me</i>	2.55	1.70	<b>2.60</b>

### 3.1 Discussion

Most of these optical gap calculations are close to experiment, with CIS being the closest method by far. TDDFT and BSE consistently underestimated the optical gap of *Bp*. Si et al. also encountered this problem with *Bp* optical gap calculations, and this is discussed in detail in Section 3.2. First some more general observations of these optical gap calculations will be addressed.

**Choice of Geometry:** By comparing Table 3.3 and Table 3.4, we clearly see that the optical gaps calculated on ground-state geometries were all much higher than those calculated on excited-state structures. These excited-state geometry calculations were an attempt to estimate the Stokes shifts of the molecules in the *Bp-F-Nap* system – the decrease in optical gap due to geometric relaxation. This attempt failed, as the resulting optical gaps are much lower than experimental values. All geometries were optimized in DFT – a ground-state theory – so it is more likely that the excited-state geometries are the cause of this error. Furthermore, it is well-known that excited-state calculations are very sensitive to geometry, and especially triplet-state calculations. For this reason, only ground-state geometries are used in the following calculations.

**Tamm-Dancoff Approximation:** All BSE calculations and most TDDFT calculations were done within the Tamm-Dancoff approximation [8], which restricts the excitation space to only transitions from occupied to virtual/unoccupied orbitals. It has been shown that

this approximation should not be applied to small systems, or systems with strong exciton localization [32], such as the systems that we are investigating. The code we used for BSE calculations – RGWBS – uses the Tamm-Dancoff approximation by default, and all attempts to run calculations without it failed. We were able to calculate TDDFT excitations without the Tamm-Dancoff approximation using Q-Chem, but this had no effect on the excitation energies.

CIS calculations were the closest to experimental values by far. However this does not indicate that CIS is a superior method; it is likely by chance that CIS accurately predicts the optical gaps of *Bp*, *F*, and *Nap*. The excitation model gets more physically accurate from CIS to TDDFT to BSE, yet the performance of these methods varies wildly. Each method has been shown to be superior for different systems [6, 31, 36], and it is very difficult to predict which model will be better for a new system. For this reason we conclude that CIS is not the superior method, but just lucky with the *Bp-F-Nap* system. Instead it is recommended to use a more complete excitation model such as TDDFT or BSE.

The failure of TDDFT and BSE at predicting the *Bp* optical gap needs to be addressed. There are many sources of error in optical gap calculations, especially for triplets. But the more common sources of error cannot account for this severe underestimation of *Bp*'s optical gap. This underestimation was reported by Si et al. in [11], and a discussion on this error follows.

### 3.2 Discussion – Benzophenone

After calculating the optical gap of benzophenone, Si et al. found that the spin and charge densities were too high on the oxygen atom. To force their calculations to better resemble experiment, Si et al. used CDFT to constrain  $-0.1e$  on benzophenone's oxygen, and one-third of the triplet spin density on benzophenone's benzene rings<sup>4</sup> [11]. Many different calculations were tested to explore why this error in Mulliken populations was occurring;

---

<sup>4</sup>This method could not be implemented using Parsec and RGWBS, so it was unable to correct these BSE calculations as they did.

these are listed below.

We find that both excited-state DFT calculations and ground-state TDDFT calculations also result in too much Mulliken charge localized on oxygen (see Table 3.6). However, excited-state TDDFT calculations find a Mulliken charge population very close to experiment, and even closer when using a water solvent model. This suggests that DFT may only predict ground-state Mulliken populations, even for excited-state calculations. This problem appears to be solved by using TDDFT excited-state calculations, and more so when using a water solvent model. However, experimental optical gaps of *Bp* do not depend on the choice of solvent, indicating that the inclusion of solvent effects is just approximating the physical effect that alters *Bp*'s charge populations. We made many attempts to find the source of this error.

**Electronic Solvent Effects:** One possible cause for this underestimation is solvent effects. When an H<sub>2</sub>O solvent model was used in TDDFT calculations, the optical gap increased by about 0.3 eV, making it much closer to experimental values. However upon closer inspection it appeared that the Mulliken charge populations were nearly unchanged after using a solvent (see Table 3.6). It appears that that TDDFT excited states correctly predict the charge population on oxygen (spin populations were unavailable in Q-Chem), but still underestimate the optical gap. It is possible that the spin populations in the TDDFT calculations are still incorrect, and that the spin constraint used by Si et al. would correctly adjust the optical gap.

Solvent effects and charge/spin constraints are clearly just rough approximations for the actual behavior of the benzophenone excitation. These calculations still underestimate the gap after including quasiparticle effects (GW) and electron-hole interactions (BSE), so another physical effect must be playing a role. The SM8 solvent model does not include for variations in the geometry due to solvent and thermal effects, and this variation in geometry may have a large effect on the excitation energy.

Table 3.6: Mulliken populations on benzophenone oxygen

	TDDFT			Lit. [11]	
	no solvent	in H2O	DFT	Pre-constraint	Post-constraint
<i>ground-state</i>	-0.43	-0.41		<b>-0.33</b>	<b>-0.10</b>
<i>triplet-state</i>	0.04	-0.04	-0.42		

**Variations in Geometry:** It has been shown in this work that excitation energies are extremely sensitive to the choice of geometry. Even small variations in the geometry can therefore have a significant impact on the excitation energy, such variations that can be caused by thermal and solvent effects. A recent computational study [37] of phenalenone (a planar molecule, see Figure 3.1) found that out-of-plane vibrational modes significantly affected energy levels. This may be explained by its molecular structure: phenalenone is planar, with an oxygen on the outer edge of the molecule. Because of this oxygen, phenalenone is very polar, which is increased in a polar solvent. This high polarity creates an electric field along the molecular plane; even small displacements out of this plane – and electric field – can cause a large change in energy.

Like phenalenone, *Bp* has a near-planar structure, and an outlying oxygen (see figure Figure 3.2 which induces a high polarity [38]). These similarities suggest that small out-of-plane displacements may also have a large effect on the energy of *Bp*. This hypothesis was tested very simply, by manually rotating the benzene rings of *Bp* and re-calculating the triplet excitation energy. Both benzene rings were rotated symmetrically, along the C-C bond between the benzene ring and the carbonyl group of *Bp*. These calculations (see Table 3.7) show that rotating the benzene rings has a very small effect on the triplet excitation energy<sup>5</sup>.

Because these rotations had such a small effect on the triplet excitation energy, it cannot be concluded that such small displacements in geometry account for the problem with TDDFT and BSE calculations. Instead, it may simply be that the hybrid and GGA

<sup>5</sup>These calculations used a different optimized geometry for *Bp*, so the energies are slightly different from those reported earlier.

Figure 3.1: Phenalenone molecule

(a) Front view

(b) Side view

Figure 3.2: *Bp* molecule

Table 3.7: Lowest triplet energy of  $Bp$ , by angle between benzene rings

Angle between benzenes	Excitation energies (eV)	
	CIS	TDDFT(B3LYP)
33.9°	2.83	2.92
54.5°(ground state geometry)	2.86	2.92
85.6°	2.92	2.98
90.8°	2.93	3.00

exchange-correlation functionals cannot calculate the correct correlation for  $Bp$ .

**CI Convergence:** CIS appears to be the best excitation method for estimating triplet excitation energies on the  $Bp$ - $F$ - $Nap$  system. However CIS excitation energies are only reliable if they are converged – that is, if including larger excited Slater determinants (doubles, triples, etc.) does not change the result. Adding larger excitations includes more correlation, and for many systems the correlation is mostly accounted for by only the single and double excitations [39] – for example, in a CISD calculation. A CISD calculation was run on  $Bp$  (see Table 3.8), which shows that these CIS energies are in fact not converged, and therefore unreliable. These calculations were done in Q-Chem, using the RI approximation [40].

Table 3.8: Lowest CIS and CISD energies of  $Bp$

triplet state	Excitation energies (eV)		
	CIS	CISD	CISD correction
1	3.11	4.03	0.92
2	3.23	4.25	1.02
3	4.15	3.57	-0.58
4	4.52	4.92	0.40

Because the CISD correction is so large, this result is not yet converged. In order to converge the CI calculations, it is necessary to add triples (CISDT), quadruples (CISDTQ), and so on, until the excitation energy is unchanged. However these calculations were not

possible with the software and computational resources currently available. Within the CISD level of accuracy, the lowest triplet state is 3.57 eV, which is about 0.6 eV higher than experiment, and about 1.0 eV above the BSE result. Therefore we cannot reconcile the CI and BSE results; these errors likely have different causes. It is still unclear why BSE does not reproduce experimental excitation energies, and the CI calculations are not yet converged.

It appears that the constrained-DFT method employed by Si et al. in [11] successfully accounted for electron correlation, which CIS, TDDFT, and BSE failed to do. However this method is very empirical, and requires very specific knowledge of the electronic structure of the system in question. There are many unanswered questions regarding these excited-state calculations, which should be addressed in a future study.

## CHAPTER 4

### COMPUTATIONAL IMPLEMENTATION: COUPLING

This chapter discusses calculations of electronic coupling for TTET in the *Bp-F-Nap* system. In particular, the Hartree-Fock method and the FSD method are studied in detail.

All geometries used in these calculations were taken from the complete *Bp-F-Nap* geometry, which was optimized into the ground electronic state, using DFT with PBE in DMol. Each fragment used in these coupling calculations was taken from this geometry, and passivated with hydrogen – but not re-optimized. For example, the *Bp-me* fragment used in these coupling calculations has the same benzophenone geometry as does *Bp-F-Nap*, and one bridging carbon, which is then passivated with hydrogen. The intention is to make this method provide the highest level of accuracy using only adiabatic states – that is, eigenstates of the systems in question.

**HF Coupling** All HF coupling energies were calculated in NWChem [41]. The process used was to:

1. Generate the ground- and triplet-state HF orbitals on the donor and acceptor fragments:  $(D|D^3)$ ,  $(D||D)$ ,  $(A||A^3)$ , and  $(A||A)$
2. Combine these orbitals into pseudo-diabatic initial and final states:  $(D, A||D^3, A)$  and  $(D, A||D, A^3)$
3. Calculate the coupling between these states.

Instead of generating these diabatic states on the donor and acceptor fragments separately, it is also possible to use CDFT to generate diabatic-like states on the complete donor-acceptor dimer. This method is not recommended, however, because often the orbitals calculated on the dimer system will be nearly orthogonal, which will make the coupling

between states artificially low.<sup>6</sup>

HF coupling results for the  $Bp \rightarrow F$  transition (see Table 4.1) are much smaller than Si's. This difference may be in part due to our using geometries optimized into the ground state, and his using CDFT with a localized triplet; however these results are so small that our methods likely differ more significantly. More importantly, these calculations were very sensitive to the choice of donor and acceptor; for this reason, HF coupling was not calculated for the rest of the Bp-F-Nap system.

The choice of basis set is also important for coupling calculations. The 6-31G\*, 6-31+G\*, DZP, and TZVP basis sets all produced similar coupling results. The only basis set that is not recommended for use in these calculations is 6-31G, which does not include polarization and cannot account for longer-range effects. For this reason, all further calculations with Q-Chem used 6-31G\*.

Table 4.1: HF coupling calculations for the  $Bp \rightarrow F$  transition (meV)

<i>donor</i> $\leftrightarrow$ <i>acceptor</i>	Basis Sets				
	6-31G	6-31G*	6-31+G*	DZP (Dunning)	TZVP
$Bp-me \leftrightarrow F$	0.57	0.25	0.25	0.22	0.25
$Bp \leftrightarrow F-me$	0.19	1.63	1.63	2.01	1.94
$Bp \leftrightarrow F$	0.05	0.48	0.48		

**FSD Couping:** Because FSD is based on adiabatic states, ground-state optimized geometries can be used. These calculations used the Q-Chem FSD function, which calculates TDA-CIS excited states; the 6-31+G\* basis set was used for all calculations. FSD is very robust under different choices of the donor and acceptor fragment, as shown in Table 4.3. However FSD still requires the user to select the proper excitations, which is not always trivial.

<sup>6</sup>Thanks are due to Huashan for pointing this out.

For this reason, FSD couplings are calculated on both two-molecule dimers, and on the entire *Bp-F-Nap* molecule. While the TDDFT excitations for FSD calculations are nearly identical for both geometries, the coupling results are very different. The coupling energies calculated on the complete *Bp-F-Nap* molecule are larger than those calculated on dimers; this is likely due to the increased orbital delocalization allowed by using the entire molecule for DFT calculations.

**FSD on Dimers:** The *Bp-F*, *F-Nap*, and *Bp-Nap* dimers were taken from the complete *Bp-F-Nap* geometry. While the *Bp-F* and *F-Nap* dimers are both complete fragments, the *Bp-Nap* dimer is simply the *Bp-me* molecule and *Nap-me* molecule separated by empty space, but in the same position and orientation as in the *Bp-F-Nap* molecule. The FSD coupling energies for these dimers are listed in Table 4.2. The SM8 solvent model [35] was also tested (with an H<sub>2</sub>O solvent), which had a significant effect on the coupling energies of the *Bp-F* and *Bp-Nap* systems. This is likely due to the polarizability of the oxygen on *Bp*<sup>7</sup>.

**FSD on the *Bp-F-Nap* Molecule:** Using the entire *Bp-F-Nap* molecule was not always successful. The TDDFT excitations were not always localized on either the bridge, donor, or acceptor; in this case it was not possible to calculate FSD coupling energies. This problem was addressed by using an H<sub>2</sub>O solvent in Q-Chem. Adding a solvent caused the TDDFT excitations to be more localized onto the bridge, donor, and acceptor, allowing for successful FSD calculations. These results are listed in Table 4.2. Because previous calculations showed that FSD is robust in the choice of donor and acceptor fragments, one donor/acceptor designation was used for each calculation.

#### 4.1 Discussion – Coupling

When calculated on two-molecule dimers, HF coupling results are much smaller than those from Si et al.. This difference is so large that there is likely a difference between our

---

<sup>7</sup>This effect was also found in the optical gap calculations of *Bp*, as discussed in Chapter 3.

Table 4.2: FSD coupling calculations, on both the complete *Bp-F-Nap* molecule, and its constituent dimers (meV)

	Dimers		Complete <i>Bp-F-Nap</i> molecule (in H2O)	Lit.[11]
	no solvent	in H2O		
<i>Bp</i> $\leftrightarrow$ <i>F</i>	0.33	1.24	2.29	<b>3.5</b>
<i>F</i> $\leftrightarrow$ <i>Nap</i>	2.66	2.90	5.71	<b>5.1</b>
<i>Bp</i> $\leftrightarrow$ <i>Nap</i>	1.32	3.71	6.47	<b>1.7</b>

Table 4.3: FSD coupling calculations for the *Bp-me* $\rightarrow$ *F* transition (meV), calculated on the *Bp-F* dimer

<i>donor</i> $\leftrightarrow$ <i>acceptor</i>	No Solvent		In H2O		Lit. [11]
	PBE	B3LYP	PBE	B3LYP	
<i>Bp-me</i> $\leftrightarrow$ <i>F</i>	0.34	1.00	1.23	2.22	
<i>Bp</i> $\leftrightarrow$ <i>F-me</i>	0.31	1.00	1.25	2.22	<b>3.5</b>
<i>Bp</i> $\leftrightarrow$ <i>F</i>	0.33	1.00	1.24	2.22	

methods, however this difference could not be identified. One possible cause is Si’s use of charge and spin constraints. As discussed in Section 3.2, Si et al. used CDFT charge- and spin-population constraints during their calculations, in order to force their DFT orbitals to mimic those observed in experiment. Because these CDFT methods were unavailable, other methods were used to investigate this disparity.

**Solvent Effects:** Solvent effects are one possible cause for DFT’s bad estimation of charge and spin populations. As done for optical gap calculations (see Section 3), an H2O solvent was added using Q-Chem; this raised the coupling energies by as much as 1 meV (see Table 4.3). However, this effect is likely due to the solvent polarizing the oxygen on Bp, pushing the orbitals closer to the center of the dimer.

**Variations in Geometry:** As discussed in Section 3.2, we propose that DFT’s bad estimation of orbitals is due to variations in *Bp* geometry that are not accounted for. This effect

will also influence the charge and spin densities on *Bp*, so it will likely have a significant effect on electronic coupling calculations involving *Bp* as well.

**Choice of Donor and Acceptor:** The HF coupling method appears to be very sensitive to choice of donor and acceptor geometry, while the FSD method does not. This is likely due to the difference in the generation of orbitals between methods. In FSD coupling, a spatial region is chosen for the donor and acceptor. Adiabatic orbitals (composed of eigenvalues of the system) are then calculated on the entire donor-acceptor molecule, and a linear combination of these is calculated to maximize the spin difference between excitons. For HF coupling, the user chooses donor and acceptor fragments, and calculates orbitals on them independently. The HF method requires the user to determine the delocalization of orbitals between the donor and acceptor – for example, whether a bridge atom will be included with the donor or acceptor, or neither. There is no established method for choosing these donor and acceptor fragments, which makes HF coupling very difficult to use empirically. In a similar way, using the complete *Bp-F-Nap* molecule increases the FSD coupling energies significantly.<sup>8</sup>

**Suggested Method:** The HF coupling method is difficult to implement without bias – as it is incredibly sensitive to the choice of donor and acceptor fragments. The FSD method is not as sensitive to the donor and acceptor designations, making it a much more robust method. FSD couplings calculated on the entire *Bp-F-Nap* molecule are used in the final TTET rate calculations – rather than on each two-molecule dimer. This limits the user influence in the calculation to choosing the donor and acceptor regions, and the results presented here have shown that the FSD method is very robust to this choice. An H<sub>2</sub>O solvent is also used in these calculations, for two reasons: first, the optical gap for benzophenone is much closer to experiment using H<sub>2</sub>O (see Chapter 3), and second, using a solvent helped localize the adiabatic orbitals onto the donor, bridge, and acceptor fragments.

---

<sup>8</sup>This was not possible with our implementation of HF coupling, because donors and acceptor orbitals needed to be calculated separately.

## CHAPTER 5

### COMPUTATIONAL IMPLEMENTATION: REORGANIZATION ENERGY

Reorganization energy must be estimated in order to calculate the Frank-Condon-weighted Density of States, and it is also used to determine the type of hopping that actually occurs. When  $\lambda \ll V_{da}$  for an EET process, coherent hopping will likely dominate, and the FGR cannot be used; if  $\lambda \approx V_{da}$ , then partially coherent hopping is likely occurring, and a different rate expression should be used [15].

The calculated reorganization energies for the  $Bp \rightarrow F$ ,  $F \rightarrow Nap$ , and  $Bp \rightarrow Nap$  transitions can be found in Table 5.1. The same calculations from Si et al. are also listed in these tables for reference. These reorganization energies validate the use of equation 2.1. Because  $\lambda$  is on the order of 0.1 eV, and electronic coupling is on the order of 1 meV,  $\lambda \gg V_{if}$ , indicating that these transition are incoherent.

Table 5.1: Reorganization energies for hopping transitions (eV)

<i>transition</i>	$\lambda_{4-point}$	$\lambda_{vib}$	<b>Lit. [11]</b>	
			$\lambda_{direct}$	$\lambda_{vib}$
<i>Bp</i> $\rightarrow$ <i>F</i>	0.67	0.68	0.82	0.94
<i>F</i> $\rightarrow$ <i>Nap</i>	0.74	0.67	0.86	0.89
<i>Bp</i> $\rightarrow$ <i>Nap</i>	0.70	0.63	0.77	0.82

### 5.1 Discussion

These calculations show that the harmonic approximation is valid for these molecules, because  $\lambda_{vib}$  is very close (within 0.1 eV) to  $\lambda_{4-point}$ [9]. This shows that our vibrational analysis can be used with the Franck-Condon weighted DOS.

These calculations of  $\lambda$  are consistently about 0.2 eV lower than Si’s estimate. This should not be interpreted as an error in my calculations or his, as there is no experimental

data of  $\lambda$  available for comparison. Instead this is likely due to using different computational packages and different XC functionals for optimization and Hessian analysis; Si used B3LYP while this study used PBE.

CHAPTER 6  
RESULTS AND DISCUSSION: TTET RATES

Using the results presented in chapters 3, 4, and 5, and Fermi’s Golden Rule (Equation 2.1) can now be used to calculate hopping rates. Two sets of results are presented: those using only ab initio calculations, and those using a corrected optical gap for *Bp* (3.11 eV). The causes for error in the *Bp* optical gap calculations are discussed in section 3.2.

### 6.1 Final FGR Parameters

For the final rate calculations, parameters calculated on ground-state PBE-optimized geometries are used, because PBE has been shown to be more accurate at optimizations and energy calculations than LDA. Although the optical gaps calculated using LDA are consistently higher than PBE (and therefore closer to experimental values), the calculated driving force is the same using both functionals. The final optical gaps, electronic couplings, and reorganization energies are listed in table Table 6.1.

Table 6.1: Final Rate Parameters

	<i>Bp</i> → <i>F</i>	<i>F</i> → <i>Nap</i>	<i>Bp</i> → <i>Nap</i>
$\Delta E_{opt}$ (eV)	-0.30	0.30	0.00
$\Delta E_{opt} - corrected$ (eV)	0.35	0.30	0.65
$V_{if}$ (meV)	2.29	5.71	6.47
$\lambda_{4-point}$ (eV)	0.67	0.74	0.70
$\lambda_{vib}$ (eV)	0.68	0.67	0.63

**Optical Gap:** The GW+BSE optical gap is used in the final rate calculations. This method is the most physically complete - accounting for both quasiparticle effects and exciton-hole interactions. CIS calculations are much closer to experimental values, however this will not always be the case. The GW+BSE gap will likely be more accurate when more effects are taken into account, as discussed in Section 3.2.

**Electronic Coupling:** FSD coupling energies calculated on the complete *Bp-F-Nap* molecule are used, calculated with an H<sub>2</sub>O solvent, and the PBE functional. These calculations allow for orbitals to delocalize across the entire molecule rather than confining them to a dimer, making them less subject to user influence. It may be more accurate to use B3LYP rather than PBE, but this functional was too computationally intensive for the resources we had available.

**Exciton-Phonon Interaction:** The reorganization energies listed in table Table 6.1 are not used explicitly in the FGR; they are listed to show the validity of the phonon decomposition of *Bp*, *F*, and *Nap*. These phonon spectra are used in the Franck-Condon weighted density of states, which accounts directly for the exciton-phonon interaction. The phonon spectra and Huang-Rhys factors for each molecule are shown in figure Figure 6.1. The FCWD is plotted for each molecule, by optical-gap driving force  $\Delta G$ , in figure Figure 6.2.

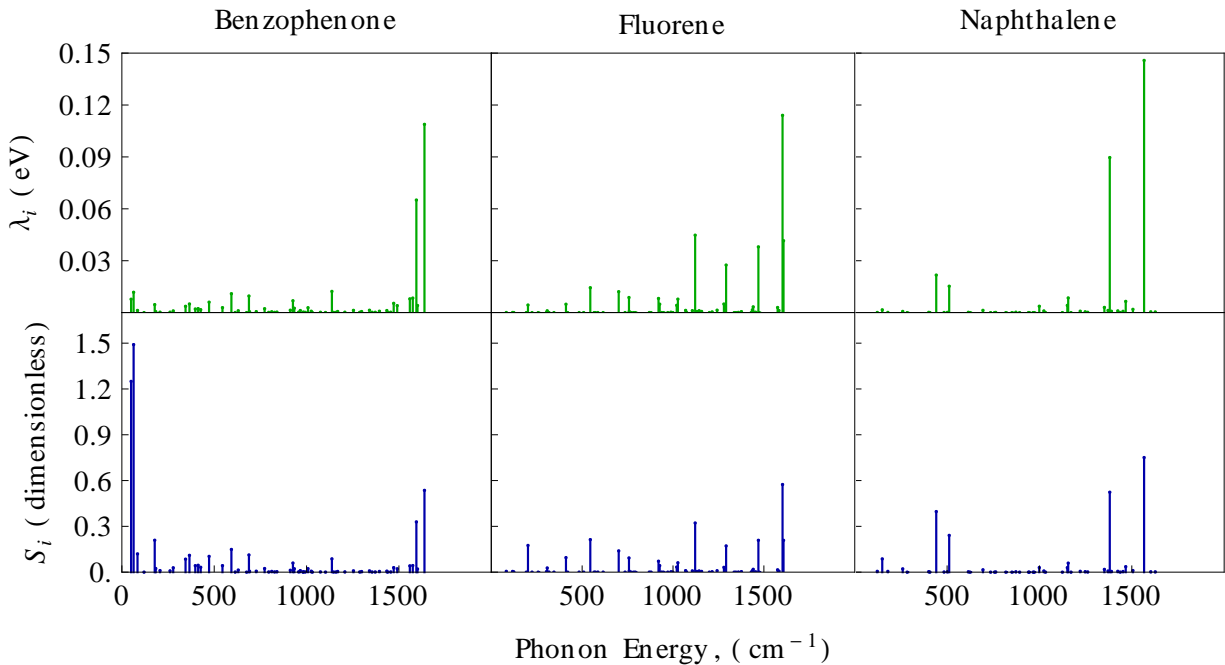


Figure 6.1: Modal reorganization energies  $\lambda_i$  and Huang-Rhys factors  $S_i$

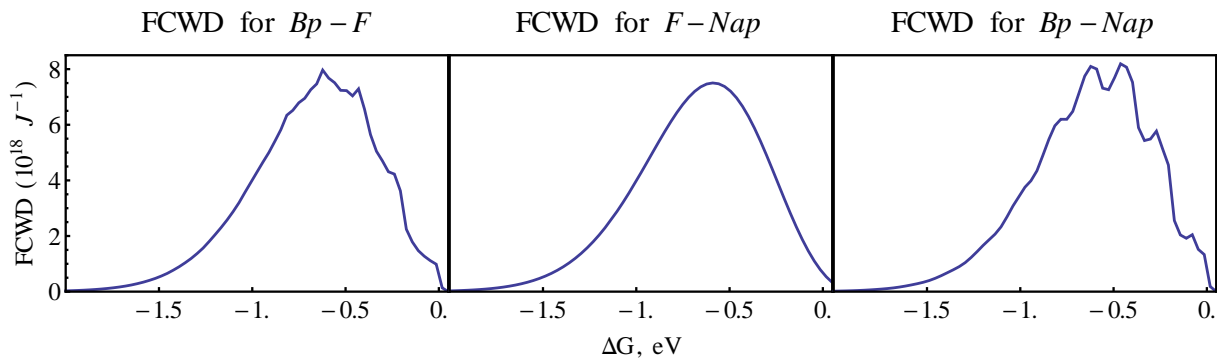


Figure 6.2: FCWD for  $Bp$ ,  $F$ , and  $Nap$

## 6.2 Final Rates and Discussion

Two sets of rates are calculated: those using only ab initio calculations, and those using calculations with a corrected optical gap for  $Bp$ . Both are listed in table Table 6.2.

Table 6.2: Final Hopping Rate Calculations, at 300K ( $10^{10}$  Hz)

	Ab initio	Using corrected $Bp$	Si et al. [11]	Expt. [10]
$Bp \rightarrow F$	4.56	5.04	<b>2.50</b>	<b>0.64</b>
$F \rightarrow Nap$	20.70	20.70	<b>8.90</b>	$\gg$ <b>0.64</b>
$Bp \rightarrow Nap$	4.00	48.00	<b>2.60</b>	<b>0.95</b>

The final rate calculations are significantly higher than both the computational and experimental benchmarks. The most likely cause for error in these calculations is the electronic coupling and the DOS. The optical gap values for the donor, bridge, and acceptor are consistent throughout literature, and these calculations are close to these literature values. However there are no experimental values to which we may compare these coupling and DOS calculations.

**Density of States:** The DOSs for each hopping step (see figure Figure 6.1) have a maximum at  $\Delta G \approx 0.6$  eV; that is, the fastest hopping should therefore occur when the donor and acceptor excitation energies differ by about 0.6 eV. The driving force for  $Bp \rightarrow Nap$  hopping

is positioned at this maximum (0.65 eV), giving it the highest  $\rho$  value of all three transitions. The other two transitions,  $Bp \rightarrow F$  and  $F \rightarrow Nap$ , have nearly equal values for  $\rho$ , which are both roughly 2/3 that of  $Bp \rightarrow Nap$ . However the final rates indicate that  $Bp \rightarrow Nap$  hopping is faster than  $Bp \rightarrow F$  by a factor of 10, which is consistent with experimental values (although these rate calculations are much higher than those in experiment). The calculations of  $\rho$  are much more robust than the calculations of  $V_{if}$ , which is likely a much greater source of error.

**Electronic Coupling:** Hopping rates in equation 2.1 are very sensitive to  $V_{if}$ ; this is because  $V_{if} \ll 1$ , and the rate is proportional to  $|V_{if}|^2$ . Even a small error in  $V_{if}$  can significantly affect the rate; this problem is complicated by the lack of experimental values, and the absence of a proven method of calculating  $V_{if}$  for TTET. These problems motivated the detailed study of electronic coupling in chapter 4. Yet even with the most robust and least empirical method available, these results are still much higher than the computational benchmark [11], and predict much higher rates than the experimental benchmark [10]. Specifically,  $V_{if}$  for the  $Bp \rightarrow Nap$  transition is much higher than that of  $Bp \rightarrow F$  and  $F \rightarrow Nap$ , which is likely unphysical due to the large separation between the  $Bp$  and  $Nap$  molecules. Electronic coupling is the least-well understood part of these rate calculations; a deeper study is clearly needed to determine the best method for calculating this value.

## CHAPTER 7

### DISCUSSION AND CONCLUSIONS

This thesis research investigated the calculation of incoherent triplet-triplet exciton transport rates on the benzophenone-fluorene-naphthalene molecule. These rates were calculated using Fermi’s golden rule, which relies on three main parameters of the system – *optical gap*, *electronic coupling*, and *density of states*. However there is little consensus on the correct methods for calculating each of these parameters, and studies in literature often contain unexplained assumptions and empirical adjustments. This thesis proposed many improvements to the calculations found in literature, and addressed the commonly-made assumptions. Of particular interest was the benzophenone molecule, which is very efficient at triplet generation, yet poses many computational challenges. It is found that the commonly-encountered problem in calculating *Bp* excitation energies is caused by small fluctuations in molecular geometry due to solvent and thermal effects. The suggestions proposed in this thesis can be expected to enhance our understanding of TTET, and better enable accurate prediction of TTET rates on new systems.

**Optical Gap:** In the literature, explanations are rarely given for the choice of method for calculating optical gaps. TDDFT and BSE – using exchange-correlation functionals like PBE and B3LYP – are commonly used with little justification. The method closest to experimental values is then decided as the best method; this interpretation is empirical, and cannot be used in predictive analyses. However even the most advanced excitation methods do not always succeed. While TDDFT and BSE produce good results for fluorene and naphthalene, they underestimate the optical gap of benzophenone, the donor molecule of the *Bp-F-Nap* system. On the other hand, the CIS excitation method matches experiment very well. This problem was also encountered by Si et al. in their work [11], and they adjusted their DFT optical gap calculations by imposing experimentally-measured charge and spin constraints.

In this study, many calculations were tested to find the source of this error within TDDFT and BSE.

Adding an electronic H<sub>2</sub>O solvent model raised the TDDFT benzophenone optical gap by 0.3 eV, much closer to experimental values; this had a similar effect to Si’s charge and spin constraints, by adjusting the benzophenone charge and spin populations. However, choosing to use this solvent model is no less empirical than Si’s constraints, making it difficult for use in predictive analyses.

Another possibility was that this underestimation of the *Bp* optical gap is due to small displacements in *Bp* caused by solvent and thermal effects. It has been shown that in phenalenone, a planar molecule similar to *Bp*, even small out-of-plane vibrational modes cause large changes in the energy [37]. Phenalenone is a very polar molecule, which induces a local electric field; these small out-of-plane displacements displace parts of the phenalenone molecule out of this electric field, causing a large change in energy.

Benzophenone is also very polar and near-planar, suggesting that out-of-plane displacements in *Bp* will have a similarly large effect on energy. However it is found that such displacements have almost no effect on the triplet excitation energy in *Bp* – even with large out-of-plane displacements.

Finally, it was found that CIS calculations, which had provided results closest to experimental values, are unconverged. When doubly-excited Slater determinants are added (a CISD calculation), the CIS excitation energies are changed by as much as 1 eV. Therefore, larger excitations (triples, quadruples, etc.) need to be added before the CI result is converged. Furthermore, the CISD triplet energy is roughly 1 eV higher than the BSE result, so we cannot conclude that these errors stem from a similar issue. It appears that the CDFT method used by Si et al. successfully accounted for electron correlation, while TDDFT, BSE, and CIS failed. A deeper study of these calculations is required to develop a reliable ab initio method for finding excitation energies.

**Electronic Coupling:** Recently, new methods for calculating TTET coupling have been proposed. Two of these methods are tested in this thesis – Hartree-Fock coupling and fragment-spin-difference (FSD) coupling. Hartree-Fock coupling is found to be very sensitive to the choice of the donor and acceptor molecular fragment, making it very sensitive to user influence. Instead it is suggested to use FSD coupling, which is found to be robust under the choice of donor and acceptor fragment.

This can be understood by the fundamental difference between HF and FSD coupling. Both methods assume that the physically correct (diabatic) initial and final states have the triplet spin density mostly localized on the donor and acceptor moiety. However, the CDFT-based HF method requires the user to choose the exact donor and acceptor regions in which the spin is localized, while the FSD method maximizes a *spin difference* between the donor and acceptor regions, allowing for spin density to be delocalized across the entire model. This may explain why FSD is more robust to the choice of donor and acceptor regions than HF.

While the FSD method is very robust to user influence, it still requires excitations to be localized on the donor, bridge, and acceptor. The initial excitations calculated for the FSD method were not well-localized, so an H<sub>2</sub>O solvent model was used to force them onto the donor, bridge, and acceptor. In the future a better method should be developed to find localized excitations.

The final coupling calculations in this work can still be improved. In particular, the calculated  $Bp$ - $Nap$  coupling is greater than that for  $Bp$ - $F$  – which is likely unphysical, as the  $Bp$  and  $Nap$  molecules are not adjacent, while  $Bp$  and  $F$  are. This result causes the  $Bp \rightarrow Nap$  hopping rate to be roughly 10 times faster than that of  $Bp \rightarrow Nap$ , which is inconsistent with experiment; this error should also be investigated more carefully.

**Choice of Geometry:** Some studies in literature use ground-state optimized geometries, while others use excited-state optimized geometries. While there are many excited-state

theories capable of optimization, the resulting geometries have not yet been proven to reflect reality. It is found that excited-state optimized geometries tend to over-estimate the decrease in energy gap due to relaxation (the Stokes shift). This error is consistent across all excitation calculation methods; for this reason, it is recommended to use only ground-state optimized geometries until an optimization method has been proven to be successful.

**Density of States:** The Franck-Condon weighted density of states was used in this thesis research, which incorporates exciton-phonon coupling within the incoherent transport regime. While this method has been used with success in the past [17], its accuracy and robustness should still be studied. Because there is no experimental data with which to compare DOS calculations, it should be compared to other DOS measures such as the MJL equation and Marcus theory

The final TTET rates calculated in this work are much higher than those measured in experiment. Because the optical gap calculations have been compared to experiment, this error is likely due to the DOS or the electronic coupling. To validate the Franck-Condon weighted DOS, a comprehensive study should compare the available DOS methods, and their utility in calculating TTET rates. Electronic coupling calculations also require further study. FSD coupling is found to be more robust and less empirical than Hartree-Fock coupling, yet there are still difficulties with this method. Mainly, the problems with excitation energy calculations also affect electronic coupling calculations. The choice of excitation method, exchange-correlation functional, basis set, and solvent models also play a role in coupling calculation methods, and these variables should be studied. The FSD coupling method also relies on the assumption that the physically correct initial and final states have the triplet spin density mostly localized on the donor and acceptor moieties, respectively. This assumption has not been stated in the literature, but it should be well understood when using FSD (or HF coupling) in rate calculations.

The *Bp-F-Nap* molecule is a perfect system to test TTET rate calculation methods. The *Bp* molecule is very important to triplet generation and transport, due to high intersystem crossing into the triplet state. This property also causes many difficulties in calculating accurate excitation energies and electronic orbitals, which have not yet been resolved. The experimental and computational work on this molecule also provides a good benchmark to which new methods may be compared. This thesis research has studied some of the challenges in calculating TTET rates on the *Bp-F-Nap* molecule, particularly in choosing which geometries to use, and identifying the most robust methods for calculating excitation energies and electronic coupling. A future study using QM/MM methods is proposed for improving excitation energy and coupling calculations. The suggestions proposed in this thesis are general – they do not apply to only *Bp-F-Nap*. This thesis has suggested improvements to calculations found in the literature, and the numerous approximations made in literature have been tested and discussed. The suggestions proposed in this thesis should be applied to new ab initio studies of TTET, to ensure that the results are as robust and unempirical as possible.

## REFERENCES CITED

- [1] Song Guo, Wanhua Wu, Huimin Guo, and Jianzhang Zhao. Room-temperature long-lived triplet excited states of naphthalenediimides and their applications as organic triplet photosensitizers for photooxidation and triplet-triplet annihilation upconversions. *The Journal of Organic Chemistry*, 77(8):3933–3943, 2012.
- [2] Devens Gust, Thomas A Moore, and Ana L Moore. Mimicking photosynthetic solar energy transduction. *Accounts of Chemical Research*, 34(1):40–48, 2001.
- [3] A Köhler and H Bässler. Triplet states in organic semiconductors. *Materials Science and Engineering: R: Reports*, 66(4):71–109, 2009.
- [4] Sina Yeganeh and Troy Van Voorhis. Triplet excitation energy transfer with constrained density functional theory. *The Journal of Physical Chemistry C*, 114(48):20756–20763, 2010.
- [5] Zhi-Qiang You and Chao-Ping Hsu. The fragment spin difference scheme for triplet-triplet energy transfer coupling. *The Journal of chemical physics*, 133:074105, 2010.
- [6] So Hirata and Martin Head-Gordon. Time-dependent density functional theory for radicals: An improved description of excited states with substantial double excitation character. *Chemical physics letters*, 302(5):375–382, 1999.
- [7] Murilo L Tiago and James R Chelikowsky. Optical excitations in organic molecules, clusters, and defects studied by first-principles greens function methods. *Physical Review B*, 73(20):205334, 2006.
- [8] Michael JG Peach, Matthew J Williamson, and David J Tozer. Influence of triplet instabilities in tddft. *Journal of chemical theory and computation*, 7(11):3578–3585, 2011.
- [9] Volkhard May and Oliver Kühn. *Charge and energy transfer dynamics in molecular systems*. John Wiley & Sons, 2008.
- [10] Josh Vura-Weis, Sameh H Abdelwahed, Ruchi Shukla, Rajendra Rathore, Mark A Ratner, and Michael R Wasielewski. Crossover from single-step tunneling to multistep hopping for molecular triplet energy transfer. *Science*, 328(5985):1547–1550, 2010.

- [11] Yubing Si, Wanzhen Liang, and Yi Zhao. Theoretical prediction of triplet–triplet energy transfer rates in a benzophenone–fluorene–naphthalene system. *The Journal of Physical Chemistry C*, 116(23):12499–12507, 2012.
- [12] C Mijoule and JM Leclercq. Theoretical investigations of the metastable triplet state of benzophenone. *The Journal of Chemical Physics*, 70:2560, 1979.
- [13] Robin M Hochstrasser, Gary W Scott, and Ahmed H Zewail. Optical, magnetic resonance, and endor studies of the  $n\pi^*$  triplet state of benzophenone in mixed crystals. *The Journal of Chemical Physics*, 58(1):393–395, 1973.
- [14] G Wäckerle, M Bär, H Zimmermann, K-P Dinse, S Yamauchi, RJ Kashmar, and DW Pratt. Optically detected magnetic resonance studies of photoexcited o-benzophenone. orbital rotation in the lowest triplet state. *The Journal of Chemical Physics*, 76:2275, 1982.
- [15] Akihito Ishizaki and Graham R Fleming. Unified treatment of quantum coherent and incoherent hopping dynamics in electronic energy transfer: Reduced hierarchy equation approach. *The Journal of chemical physics*, 130:234111, 2009.
- [16] Max Born and Robert Oppenheimer. Zur quantentheorie der molekeln. *Annalen der Physik*, 389(20):457–484, 1927.
- [17] Huashan Li, Zhigang Wu, and Mark Lusk. Double super-exchange in silicon quantum dots connected by short-bridged networks. *Bulletin of the American Physical Society*, 58, 2013.
- [18] A Sellinger H Li, Z Wu and M Lusk. Double superexchange in quantum dot mesomaterials. *Energy & Environmental Science*, In review.
- [19] Hans R Griem. Principles of plasma spectroscopy. *Proceedings of the Physical Society*, 1, 2005.
- [20] David L Dexter. A theory of sensitized luminescence in solids. *The Journal of Chemical Physics*, 21:836, 1953.
- [21] Yihan Shao, Laszlo Fusti Molnar, Yousung Jung, Jörg Kussmann, Christian Ochsenfeld, Shawn T Brown, Andrew TB Gilbert, Lyudmila V Slipchenko, Sergey V Levchenko, Darragh P O'Neill, et al. Advances in methods and algorithms in a modern quantum chemistry program package. *Physical Chemistry Chemical Physics*, 8(27):3172–3191, 2006.

- [22] Alexander A Voityuk and Notker Rösch. Fragment charge difference method for estimating donor–acceptor electronic coupling: Application to dna  $\pi$ -stacks. *The Journal of chemical physics*, 117:5607, 2002.
- [23] Tao Liu and Alessandro Troisi. Absolute rate of charge separation and recombination in a molecular model of the p3ht/pcbm interface. *The Journal of Physical Chemistry C*, 115(5):2406–2415, 2011. doi: 10.1021/jp109130y. URL <http://pubs.acs.org/doi/abs/10.1021/jp109130y>.
- [24] W. Kohn and L. J. Sham. Self-consistent equations including exchange and correlation effects. *Phys. Rev.*, 140:A1133–A1138, Nov 1965. doi: 10.1103/PhysRev.140.A1133. URL <http://link.aps.org/doi/10.1103/PhysRev.140.A1133>.
- [25] Nathan Argaman and Guy Makov. Density functional theory: An introduction. *American Journal of Physics*, 68:69, 2000.
- [26] Yue Wang and John P. Perdew. Correlation hole of the spin-polarized electron gas, with exact small-wave-vector and high-density scaling. *Phys. Rev. B*, 44:13298–13307, Dec 1991. doi: 10.1103/PhysRevB.44.13298. URL <http://link.aps.org/doi/10.1103/PhysRevB.44.13298>.
- [27] John P. Perdew, Kieron Burke, and Matthias Ernzerhof. Generalized gradient approximation made simple. *Phys. Rev. Lett.*, 77:3865–3868, Oct 1996. doi: 10.1103/PhysRevLett.77.3865. URL <http://link.aps.org/doi/10.1103/PhysRevLett.77.3865>.
- [28] Chengteh Lee, Weitao Yang, and Robert G Parr. Development of the colle-salvetti correlation-energy formula into a functional of the electron density. *Physical Review B*, 37(2):785, 1988.
- [29] Lars Hedin. New method for calculating the one-particle green’s function with application to the electron-gas problem. *Physical Review*, 139(3A):A796, 1965.
- [30] Lars Jonsson W. G. Aulbur and John W. Wilkins. Quasiparticle calculations in solids. 2000. URL [http://en.wikipedia.org/wiki/GW\\_approximation](http://en.wikipedia.org/wiki/GW_approximation).
- [31] Murilo L Tiago and James R Chelikowsky. First-principles gw–bse excitations in organic molecules. *Solid state communications*, 136(6):333–337, 2005.
- [32] Yuchen Ma, Michael Rohlfing, and Carla Molteni. Modeling the excited states of biological chromophores within many-body greens function theory. *Journal of Chemical Theory and Computation*, 6(1):257–265, 2009.

- [33] Andreas Dreuw and Martin Head-Gordon. Single-reference ab initio methods for the calculation of excited states of large molecules. *Chemical reviews*, 105(11):4009–4037, 2005.
- [34] Bernard Delley. An all-electron numerical method for solving the local density functional for polyatomic molecules. *The Journal of chemical physics*, 92:508, 1990.
- [35] Aleksandr V Marenich, Ryan M Olson, Casey P Kelly, Christopher J Cramer, and Donald G Truhlar. Self-consistent reaction field model for aqueous and nonaqueous solutions based on accurate polarized partial charges. *Journal of Chemical Theory and Computation*, 3(6):2011–2033, 2007.
- [36] Stefan Grimme and Ekaterina I Izgorodina. Calculation of 0–0 excitation energies of organic molecules by cis (d) quantum chemical methods. *Chemical physics*, 305(1):223–230, 2004.
- [37] Martha C Daza, Markus Doerr, Susanne Salzmann, Christel M Marian, and Walter Thiel. Photophysics of phenalene: quantum-mechanical investigation of singlet–triplet intersystem crossing. *Physical Chemistry Chemical Physics*, 11(11):1688–1696, 2009.
- [38] Herbert C Georg, Kaline Coutinho, and Sylvio Canuto. Solvent effects on the uv-visible absorption spectrum of benzophenone in water: A combined monte carlo quantum mechanics study including solute polarization. *Journal of Chemical Physics*, 126(3):034507, 2007.
- [39] Attila Szabo and Neil S Ostlund. *Modern quantum chemistry: introduction to advanced electronic structure theory*. DoverPublications. com, 1989.
- [40] Florian Weigend, Marco Häser, Holger Patzelt, and Reinhart Ahlrichs. Ri-mp2: optimized auxiliary basis sets and demonstration of efficiency. *Chemical physics letters*, 294(1):143–152, 1998.
- [41] Marat Valiev, Eric J Bylaska, Niranjana Govind, Karol Kowalski, Tjerk P Straatsma, Hubertus JJ Van Dam, Dunyou Wang, Jarek Nieplocha, Edoardo Apra, Theresa L Windus, et al. Nwchem: a comprehensive and scalable open-source solution for large scale molecular simulations. *Computer Physics Communications*, 181(9):1477–1489, 2010.